04-53-13

Journal of Nuclear Materials 118 (1983) 224–233
North-Holland Publishing Company

CREEP OF STRESS-RELIEVED Zry-4 AT 673 K

F. POVOLO

Comisión Nacional de Energía Atómica, Dto. de Materiales, Av. del Libertador 8250, (1429) Buenos Aires; Comisión de Investigaciones Científicas de la Provincia de Buenos Aires, Argentina

and

A.J. MARZOCCA

Comisión de Investigaciones Científicas de la Provincia de Buenos Aires, Argentina

Received 1 February 1983; accepted 9 May 1983

Creep data, at 673 K, up to times of about 400 h and stresses between 120 and 242 MPa, in flat specimens of Zry-4 stress-relieved for 1 h at 813 K, are presented. The creep curves, when viewed in a $\log\sigma - \log\dot{\epsilon}$ diagram, show a scaling behaviour leading to a master curve similar to the one obtained in 64% cold-worked material. The data are interpreted in terms of a constitutive equation based on a creep model involving jog-drag and cell-formation, and the apparent activation energy was found to be independent of stress with a value close to the one found in the cold-worked material.

1. Introduction

The fundamental aspects of the creep characteristics of zirconium and zirconium alloys have been reviewed in detail by Lucas [1]. More recently, Novák and Hamerský [2] performed measurements of the stress sensitivity parameter, m, during creep of Zr + 4.5% Sn + 1% Mo in the temperature interval 300 to 750 K. m was found to be independent of stress, except for the highest temperature, where m increased with the applied stress. The activation area decreased with the applied stress as σ^{-1} but, at the highest temperature, it was found that the activation area increased with the applied stress, which cannot be explained using the usual dislocation glide models. Dynamic strain aging was believed to be responsible for the phenomena observed.

MacEwen et al. [3] studied the creep behaviour of specimens of α-Zr in the temperature range 870 to 975 K. Q decreased on increasing the applied stress and the stress exponent increased from 3 at low stresses to about 9 at high stresses. The results were found to be incompatible with a simple power-law representation of the steady-state creep rate in which the stress exponent is constant and $Q = U_d$, independent of stress. Keusseyan et al. [4] performed load relaxation tests on Zircaloy-2 and Zircaloy-4 with varied textures and microstructures, to study the effects of fabrication variables. A contribution to the relaxation due to dislocation climb and, possibly, of grain boundary relaxation was found at 673 K.

Povolo and Marzocca [5,6] have recently reported creep and stress relaxation data, at 673 K, in 64% cold-worked Zircaloy-4. It was shown that the log stress versus log strain rate creep curves, obtained at different strain levels, were related by scaling, leading to a master curve similar to the one obtained by stress-relaxation in bending, in the same material and at the same temperature. The master curve, obtained by translation on the individual creep curves, had the typical form for a constant hardness log stress versus log strain rate curve at high homologous temperatures [7]. Furthermore, it was shown that the log stress versus log strain rate creep curves could be described by Hart's [7,8] phenomenological equation

$$\dot{\epsilon} = \dot{\epsilon}^*[-\ln(\sigma/\sigma^*)]^{-1/\lambda}, \tag{1}$$

where σ is the applied stress, $\dot{\epsilon}$ the plastic strain rate, σ^* is the hardness parameter, λ is a temperature independent parameter and $\dot{\epsilon}^*$ is a parameter which depends on temperature, heat treatment and deformation. It was also shown that the $\log\sigma - \log\dot{\epsilon}$ creep curves, in cold-worked material, could be described by the constitutive

0022-3115/83/0000–0000/$03.00

equation [6]

$$\dot{\epsilon} = B(\alpha\sigma)^n \sinh(\alpha\sigma), \quad (2)$$

where $n = 3$ and B and α are parameters that depend on strain during transient creep. It must be pointed out that eq. (2) is based on the Barrett–Nix model for creep [9] controlled by the thermally assisted motion of jogged screw dislocations and that Povolo and Marzocca [10] have discussed the interrelation between eqs. (1) and (2) in detail.

The general scaling conditions for eqs. (1) and (2) have been given by Povolo and Marzocca [10]. It was shown that λ and n must be the same for all the individual creep and stress relaxation curves if eq. (1) or eq. (2) shows a scaling behaviour in a $\log\sigma$–$\log\dot{\epsilon}$ diagram. Furthermore, Povolo and Rubiolo [12,13] have shown that these constitutive equations are plastic equations of state, for constant λ and n, only in a certain range of σ and $\dot{\epsilon}$ even if a scaling relationship is present.

It is the purpose of this paper to present creep data, at 673 K, in stress-relieved Zircaloy-4 for various applied stresses. The results will be interpreted in terms of a constitutive equation based on a creep model involving jog-drag and cell-formation. Finally, the results will be compared with those obtained for cold-worked material, interpreted within the same theoretical model and several dislocation parameters will be obtained from the experimental creep curves.

2. Results

The experimental procedure for the creep tests and the composition of the alloy used was described in ref. 5. The only change is that the 64% cold-rolled specimens were stress-relieved for 1 h at 813 K, in high vacuum, prior to the creep experiments. The texture after this treatment, as determined by the Schulz technique, is indicated by the (0002) pole figure shown in fig. 1. Fig. 2 shows the creep strain as a function of time, for stresses between 120 and 250 MPa. It was not possible to obtain creep curves for stresses higher than about 250 MPa since the specimen broke almost instantaneously above this stress level. These results suggest the usual separation between transient or primary and secondary or steady state creep, since the strain rate decreases to a constant value at all stresses. When the data are plotted as $\log\sigma$ versus $\log\dot{\epsilon}$, however, a smooth behaviour is found. This is shown in fig. 3, where $\dot{\epsilon}$ has been obtained by calculating the derivatives of the curves of fig. 2 at different strains and plotting them as a function of the corresponding stress. It can be seen

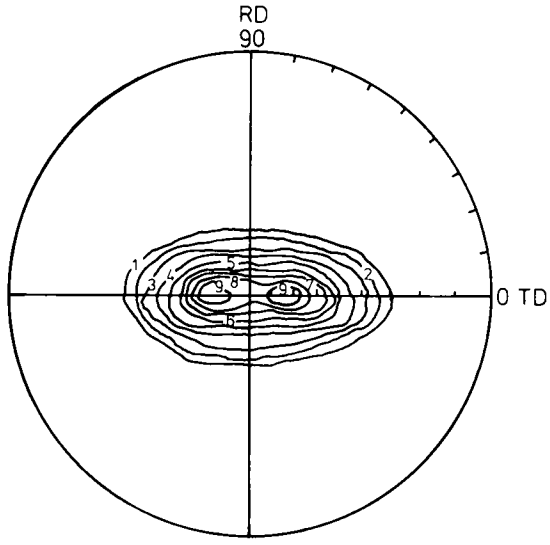

Fig. 1. (0002) pole figure for the stress-relieved Zircaloy-4.

that the $\log\sigma$–$\log\dot{\epsilon}$ curves shift to higher stresses and strain rates as the strain increases, but the shape is maintained. As for the cold-worked material, this suggests that the different curves might be related by scaling [7,8], i.e., it is possible to superimpose by translation ($\Delta\log\sigma$, $\Delta\log\dot{\epsilon}$) any one of the curves onto any of the others in such a way that the overlapping segments match within experimental error. This is shown in fig. 4, where all the curves have been superimposed to the curve for $\epsilon = 0.5\times10^{-2}$ along the translation path represented by the straight line of slope

$$\mu = \Delta\log\sigma/\Delta\log\dot{\epsilon} = 0.035. \quad (3)$$

The apparent activation energy,

$$Q = |-\partial\ln\dot{\epsilon}/\partial(1/kT)|_\sigma \approx |-\Delta\ln\dot{\epsilon}/\Delta(1/kT)|_\sigma,$$

was measured by abrupt and small changes in temperature at various stresses. It was found to be almost independent of the applied stress, in the range considered, with an average value

$$Q = (300 \pm 10)\ \text{kJ/mol},$$

which is similar to the value measured in the cold-worked material, (288 ± 6) kJ/mol.

By abrupt changes of stress, it was possible to measure the parameter

$$m = (\partial\ln\dot{\epsilon}/\partial\ln\sigma)_T \approx (\Delta\ln\dot{\epsilon}/\Delta\ln\sigma)_T \quad (4)$$

at different stress levels. The values obtained are given in table 1 where the stress, strain rate and strain, measured before the small change in stress, are also

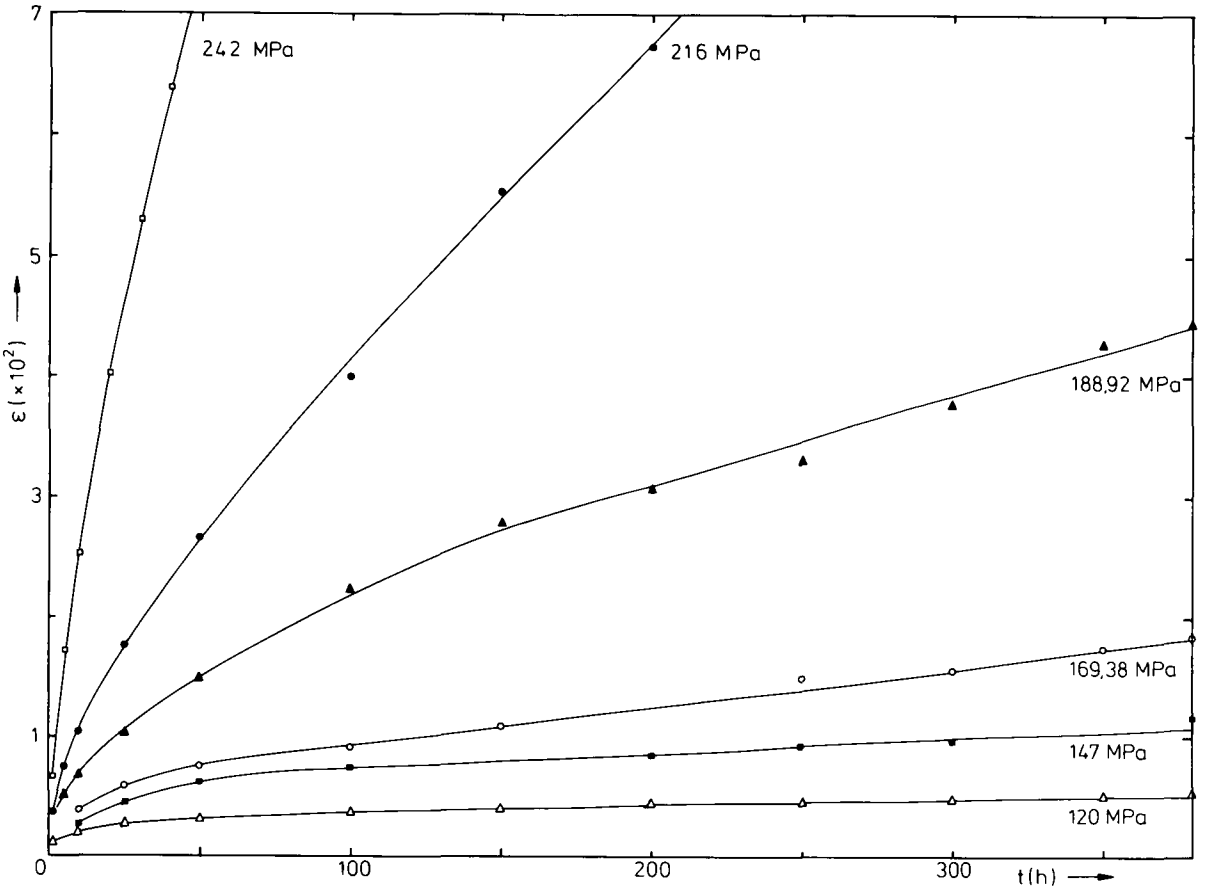

Fig. 2. Creep strain as a function of time at 673 K and various stresses for stress-relieved Zircaloy-4. Specimen cut with the axis along the rolling direction.

indicated. All the measurements have been performed in the steady state region of the strain versus time curves.

The possible contribution of grain-boundary sliding to the deformation has been determined by means of a grain counting technique proposed by Rachinger [14].

Table 1
The parameter m given by eq. (4) measured at various stresses. The stress, strain rate and strain, before the small change in stress, are indicated

m	σ (MPa)	$\dot{\epsilon}$ (s^{-1})	$\epsilon \times 10^{-2}$
6.50	120	$1.11\ 10^{-9}$	0.70
8.68	147	$3.33\ 10^{-9}$	1.74
11.10	169.4	$8.64\ 10^{-9}$	2.80
12.66	189	$1.29\ 10^{-8}$	6.56
19.87	208.2	$5.57\ 10^{-8}$	7.25
21.40	216	$5.37\ 10^{-8}$	8.26

The average relative grain elongation is

$$e_g = (La_0/L_0a)^{2/3} - 1,$$

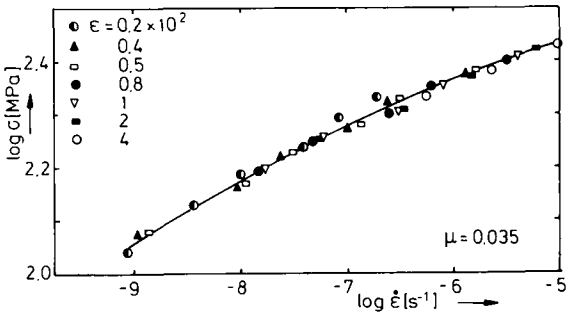

Fig. 4. Master log σ versus log $\dot{\epsilon}$ curve, obtained by superposing the curves of fig. 3 to the curve for $\epsilon = 0.5 \times 10^{-2}$, along the translation path of slope $\mu = 0.035$.

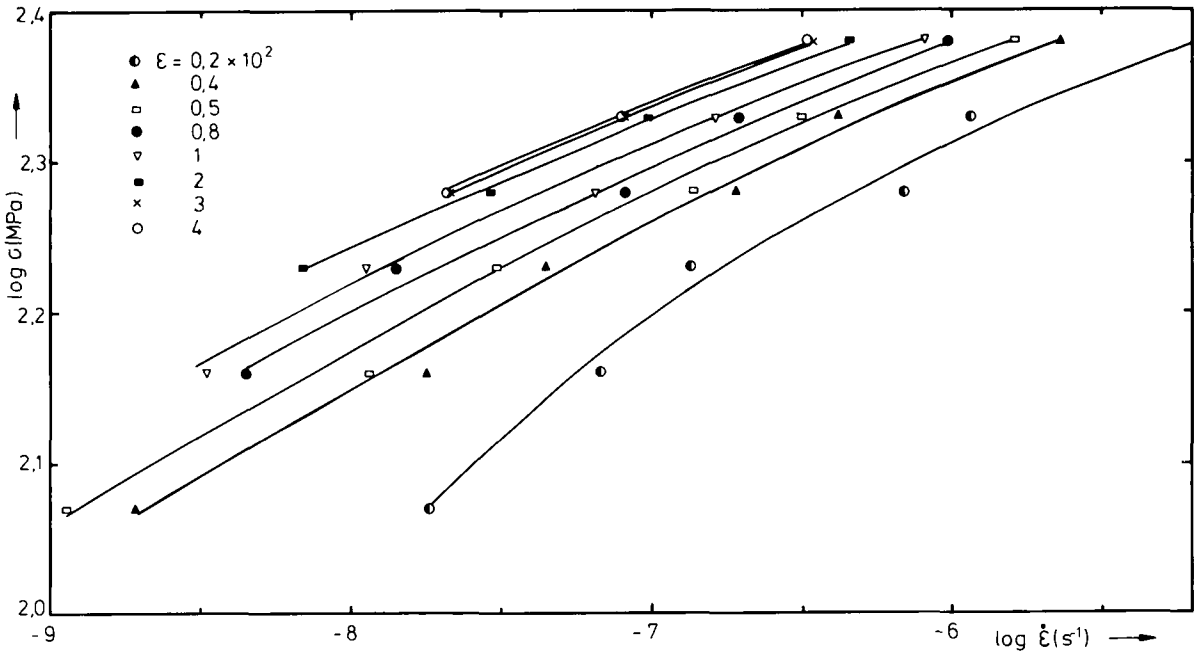

Fig. 3. Stress versus strain rate curves at different strain levels obtained from the data of fig. 2.

where L_0 and L are the average dimensions of the grains in the longitudinal direction, before and after the deformation, respectively; a_0 and a are the same quantities but in the transversal direction of the specimen. The true strain due to grain elongation is

$$\epsilon_g = \ln(1 + e_g) = \ln(La_0/L_0a)^{2/3}$$

and the total strain measured in the specimen is given by

$$\epsilon = \epsilon_g + \epsilon_{gs},$$

where ϵ_{gs} is the contribution due to grain-boundary sliding to the total deformation. The ratio

$$\gamma = \epsilon_g/\epsilon \tag{5}$$

gives the relative contribution of grain elongation to the deformation and

$$\gamma_s = 1 - \gamma = \epsilon_{gs}/\epsilon \tag{6}$$

gives the relative contribution due to grain-boundary sliding. Table 2 shows the results obtained, in various specimens crept at different initial stresses, by optical metallography. The strains where the test was interrupted are also included. γ, given by eq. (5), is shown as a function of the applied stress in fig. 5. It can be seen that the contribution due to grain-boundary sliding to the deformation is small, reaching a maximum value of the order of 14% at the highest stress.

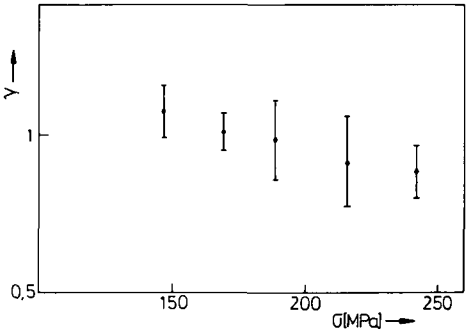

Fig. 5. Relative contribution due to grain elongation to the creep strain versus the applied stress.

3. Discussion

The master curve of fig. 4 can be described analytically by the constitutive equation

$$\alpha\sigma = (\dot{\epsilon}/\dot{\epsilon}^*)^{1/3} + \sinh^{-1}\left[(\dot{\epsilon}/\dot{\epsilon}^*)^{1/3}\beta\right], \tag{7}$$

Table 2
Relative contribution due to grain-boundary sliding to the deformation, obtained by using eq. (6): $a_0 = 9.48\ \mu m$ and $L_0 = 7.22\ \mu m$

σ (MPa)	ϵ ($\times 10^{-4}$)	L (μm)	a (μm)	ϵ_g ($\times 10^{-4}$)	γ_s (%)
147	193.7	9.7 ± 0.8	7.2 ± 0.4	211 ± 19	–
169.4	302.4	9.9 ± 0.3	7.2 ± 0.5	307 ± 20	–
188.9	697.5	10.6 ± 0.8	7.3 ± 1.1	686 ± 108	2
216	848.6	11.8 ± 2.0	8.0 ± 0.8	753 ± 133	11
242	1561.5	10.8 ± 0.9	6.7 ± 0.6	1350 ± 152	14

where

$$\beta = G^2ABK^6; \tag{8}$$

$$\dot{\epsilon}^* = B(kT)^3K^6/b^6l^3 \tag{9}$$

$$\alpha = b^2l/kT; \tag{10}$$

$$B = c_jD_vb/G^2kT; \tag{11}$$

$$A = b^2/20\alpha D_v; \tag{12}$$

where b is the Burgers vector, G is the shear modulus, D_v is the volume self-diffusion coefficient, l is the distance between neighbouring jogs on dislocations, c_j is the thermal jogs concentration, K is the ratio of cell diameter to dislocation spacing, k is Boltzmann's constant and T the absolute temperature. Eq. (7) was given by Gittus [15] and takes into account the effects of jog-drag and cell-formation upon the rate of creep. This equation is plotted in fig. 6 as $\log(\alpha\sigma)$ versus $\log(\dot{\epsilon}/\dot{\epsilon}^*)$, for different values of β. Since figs. 4 and 6 are plotted on the same scales, by superimposing both figures and translating along the axes (without rotations) [16] it can easily be seen that the master creep curve of fig. 4 can be matched to one of the curves of fig. 6. The parameters α and $\dot{\epsilon}^*$ can be obtained from the coincidence of some value of $\log\sigma$ and $\log\dot{\epsilon}$ from the experimental curve with the corresponding $\log(\alpha\sigma)$ and $\log(\dot{\epsilon}/\dot{\epsilon}^*)$ values from the theoretical one. The parameter β is read directly.

Eq. (7) was deduced by Gittus under steady-state conditions but the master curve of fig. 4 also includes data taken in the transient creep regime. It is shown in the Appendix that Gittus equation may also be valid during transient creep. When the master curve of fig.4 is superimposed to the normalized plot of eq. (7), given in

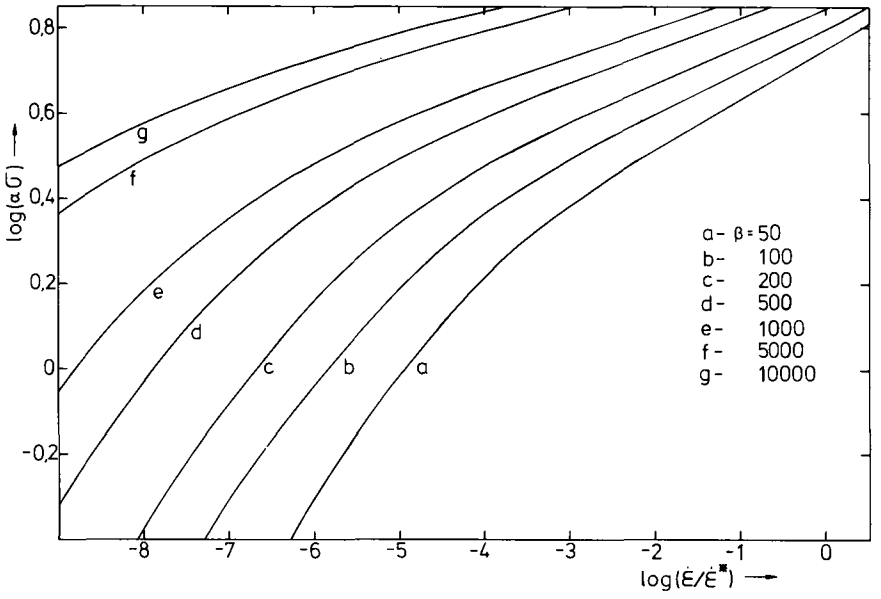

Fig. 6. Normalized plot of eq. (7).

fig. 6, to obtain the parameters α, $\dot{\epsilon}^*$ and β, it is implicitly assumed that β is constant for all the individual curves of fig. 3. On taking into account the scaling conditions for eq. (7) [11,17] it can be shown that $\mu = \frac{1}{2}$ if β has the same value for all the individual curves. As indicated in fig. 4, however, the experimental value for the slope of the translation path is 0.035, which means either that the data cannot be described by eq. (7) or that β is variable. In fact, as shown by Povolo et al. [17,18] when

$$\sinh^{-1}\left[\beta(\dot{\epsilon}/\dot{\epsilon}^*)^{1/3}\right] \gg (\dot{\epsilon}/\dot{\epsilon}^*)^{1/3}$$

and

$$\sinh(\alpha\sigma) \approx \tfrac{1}{2}\exp(\alpha\sigma)$$

eq. (7) reduces to

$$(\dot{\epsilon}/\dot{\epsilon}^*) = (1/8\beta^3)\exp(3\alpha\sigma). \tag{13}$$

Eq. (13), which is a limiting form of eq. (7), can lead to a scaling behaviour with variable β in a $\log\sigma$–$\log\dot{\epsilon}$ diagram and the scaling conditions are [17]

$$\Delta \log \alpha = -\mu \log \dot{\epsilon}, \tag{14}$$

$$\Delta \log \dot{\epsilon}^* = (3\mu - \tfrac{1}{2})\Delta \log \dot{\epsilon}, \tag{15}$$

$$\Delta \log \beta = (\mu - \tfrac{1}{2})\Delta \log \dot{\epsilon}, \tag{16}$$

which leads to $\Delta \log \beta = 0$ for $\mu = \frac{1}{2}$. The parameters of the individual $\log\sigma$–$\log\dot{\epsilon}$ creep curves of fig. 3 cannot be obtained by superimposing them to the normalized plot of eq. (7) since they are too short and the parameters cannot be unambiguously determined. This is not the case for the master curve of fig. 4 where the experimental range is extended.

If eq. (7) reduces to eq. (13), then a plot of the data of fig. 3 as $\ln\dot{\epsilon}$ versus σ, at different strain levels, gives straight lines of slope 3α and intercept $\dot{\epsilon}^*/8\beta^3$. Furthermore, on combining eqs. (14) to (16) it is easy to show that

$$\dot{\epsilon}^*/\beta^3 = C_1(\alpha)^{-1/\mu}, \tag{17}$$

where C_1 is a constant. The data of fig. 3 give straight lines when plotted as $\ln\dot{\epsilon}$ versus σ. In addition, as suggested by eq. (17) a plot of $\log(\dot{\epsilon}^*/\beta^3)$ versus $\log\alpha$ should give a straight line of slope $-1/\mu$. This last plot allows a very accurate determination of the slope of the translation path. The value $\mu = 0.035$ was obtained by using this procedure.

From eqs. (8) to (12) it is easy to show that

$$\beta = G^2b^2\dot{\epsilon}^*\alpha^2/20D_v \tag{18}$$

so that once α and $\dot{\epsilon}^*/\beta^3$ are known, $\dot{\epsilon}^*$ and β can be calculated by using eq. (18). The problem is that eq. (18) involves D_v and there is some disagreement in the literature about the self-diffusion coefficient of zirconium [19], which can give differences of various orders of magnitude between the self-diffusion coefficients extrapolated to 673 K. In this situation, the following procedure was preferred: α is determined, for the individual curve for $\epsilon = 0.5 \times 10^{-2}$, from the slope of the linear plot of $\ln\dot{\epsilon}$ versus σ, as suggested by eq. (13). Since all the curves were translated onto the curve for $\epsilon = 0.5 \times 10^{-2}$ the master curve is described by using the same parameters as for this individual curve. Once α is known, the procedure of superimposing figs. 4 to fig. 6 can only be done by a translation parallel to the $\log(\dot{\epsilon}/\dot{\epsilon}^*)$ axis, reducing the error in the determination of $\dot{\epsilon}^*$ and β. The method just described gives for the parameters of the master curve

$$\alpha = 18.84 \times 10^{-2}\,(\mathrm{MPa})^{-1}; \qquad \dot{\epsilon}^* = 1.54 \times 10^{-4}\,\mathrm{s}^{-1};$$
$$\beta = 187. \tag{19}$$

Eq. (18) can now be used to calculate D_v, with $G = 26$ GPa and $b = 3.23 \times 10^{-10}$ m, leading to

$$D_v = 1.03 \times 10^{-21}\,\mathrm{m}^2\,\mathrm{s}^{-1} \qquad \text{at 673 K.} \tag{20}$$

A similar value (1.29×10^{-21} m^2 s^{-1}) was obtained from creep data for cold-worked material [17], by using the same procedure. This value seems to be confirmed by recent measurements of the self-diffusion coefficient using the ion-beam-sputtering techniques [20]. Once D_v is known, the parameters given by eq. (19) can be compared with the values obtained from the plot $\ln\dot{\epsilon}$ versus σ for the individual curve for $\epsilon = 0.5 \times 10^{-2}$ and using eq. (18). This procedure gives

$$\alpha = 18.84 \times 10^{-2}\,(\mathrm{MPa})^{-1}; \qquad \dot{\epsilon}^* = 1.84 \times 10^{-4}\,\mathrm{s}^{-1};$$
$$\beta = 220.65,$$

which are quite similar to the values given by eq. (19). It is clear that the experimental $\log\sigma$–$\log\dot{\epsilon}$ creep curves are described by eq. (13).

The parameters for the rest of the individual curves of fig. 3 can be obtained by using the corresponding linear plots of $\ln\dot{\epsilon}$ versus σ, eq. (18) and D_v given by eq. (20). Similar values should be obtained by using the translation conditions given by eqs. (14) to (16). In fact, once α, $\dot{\epsilon}^*$ and β are known for one of the individual curves (for example the values given by eq. (19) for the curve for $\epsilon = 0.5 \times 10^{-2}$) since the increments $\Delta \log\dot{\epsilon}$, needed to translate the individual curves, can be easily determined, eqs. (14) to (16) can be used to obtain $\Delta \log\alpha$, $\Delta \log\dot{\epsilon}^*$ and $\Delta \log\beta$ and, consequently, to obtain the parameters for the rest of the individual curves from those of the reference curve ($\epsilon = 0.5 \times 10^{-2}$). The

detailed procedure is given elsewhere [17] but it should be pointed out that complete agreement is obtained with the values given by the $\ln \dot{\epsilon}$ versus σ plots. The average experimental curves of fig. 3 can be described with eq. (7) with a maximum deviation of the order of 2%.

The average distance between neighbouring jogs and the ratio of cell diameter to dislocation spacing can be obtained, at each strain level, from α, $\dot{\epsilon}^*$ and β by using eqs. (8) to (12) and c_j given by [21]

$$c_j = \exp(-xGb^3/kT), \qquad (21)$$

$$0.2 > x \geq (1/8\pi),$$

which on taking $G = 26$ GPa, $b = 3.23 \times 10^{-10}$ m, $T = 673$ K and $x = 1/8\pi$ leads to

$$c_j = 2.35 \times 10^{-2}.$$

K and l are plotted, as a function of strain, in fig. 7. The values obtained through a similar procedure, for the creep data in the 64% cold-worked specimens reported in ref. 17, are also included. It can be seen that both l and K increases at low strains, saturating for large deformations.

The K values shown in fig. 7 are of the order of magnitude of those obtained by observations of the microstructure in severals metals and alloys [22] and lie in the range predicted theoretically by Gittus [23], i.e., $20 > K > 5$. Similar values were obtained, in the same alloy and at the same temperature, from data of stress relaxation in bending. As shown by fig. 7, larger values are obtained for the average distance between neighbouring jogs for the stress-relieved specimens as compared to the cold-worked ones. This might be due to the fact that the starting dislocation density is lower after the stress-relieving treatment and, consequently, the average distance between jogs is higher. Furthermore, l increases slightly with the creep strain for both types of specimens. A possible explanation for this behaviour might be the fact that an interaction between jogs occurs at high strains, leading to annihilation processes. In fact, it is assumed in Gittus model that l depends only on the thermal jogs concentration which is clearly an oversimplification. In any case, as shown by fig. 7, l changes only by one Burgers vector from low to high strains and this variation should be considered with caution.

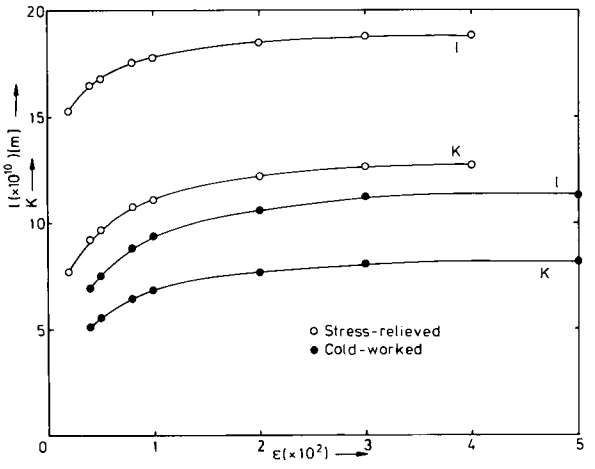

Fig.7. Average spacing between neighbouring jogs, l, and ratio of cell diameter to dislocation spacing, K, as a function of the creep strain.

K also increases with increasing creep strain in both types of specimens. This should be expected since according to Holt [24]

$$D = K\rho_t^{-1/2}, \qquad (22)$$

where ρ_t is the total dislocation density and D is the cell diameter. In addition

$$\rho_t = \rho + \rho_{sb},$$

where ρ_{sb} is the dislocation density in the cell boundary and ρ the density of within-cell dislocations. ρ increases in the primary creep region, immediately after the application of the load, and then decreases to a saturation value in the steady-state regime; ρ_{sb} increases rapidly from the primary to the steady-state region, toward a saturation value. Since ρ_{sb} varies more than ρ the total dislocation density increases on going from the primary to the steady-state regime. Evidence for this behaviour can be found in ref. 22 and refs. 25 to 29. Then, from eq. (22)

$$K = D\rho_t^{1/2}$$

and since D decreases only slightly and ρ_t increases more on going from the primary to the steady-state creep, K should increase with creep strain toward a saturation value. This is the behaviour shown in fig. 7.

On differentiating eq. (7) it is easy to show that the parameter m, defined by eq. (4), is given by

$$m = 3\alpha\sigma(\dot{\epsilon}/\dot{\epsilon}^*)^{-1/3}\left\{1 + \beta/\left[1 + \beta^2(\dot{\epsilon}/\dot{\epsilon}^*)^{2/3}\right]^{1/2}\right\}^{-1}. \qquad (23)$$

This equation shows that m depends on the applied stress, on the strain rate and on the parameters α, $\dot{\epsilon}^*$ and β or, which is equivalent, on K and l. Since α, $\dot{\epsilon}^*$ and β are known as a function of strain, eq. (23) can be used to calculate the predicted m values which can be compared with the measured ones, given in table 1.

Table 3
Comparison between the measured values for the parameter m, m_{exp}, and the values predicted by eq. (23), m_{th}

σ (MPa)	$\dot{\epsilon}$ (s^{-1})	$\epsilon \times 10^{-2}$	$\alpha \times 10^{-3}$ (MPa^{-1})	$\dot{\epsilon}^* \times 10^{-4}$ (s^{-1})	β	m_{exp}	m_{th}
120	8.33×10^{-10}	0.70	19.45	2.23	228.4	6.8	7.1
147	3.33×10^{-9}	1.74	20.59	4.29	623.7	8.7	8.9
169.4	8.06×10^{-9}	2.80	21.05	5.32	807.2	10.3	10.4
188.9	1.31×10^{-8}	6.56	21.12	5.60	855.4	11.0	11.6

Such a comparison is made in table 3, where the strain rate, the stress and the strain level, before the small change in stress, and the parameters α, $\dot{\epsilon}^*$ and β are indicated. m_{th} are the values predicted by eq. (23) and m_{exp} those obtained by making a small change in the applied stress ($\Delta\sigma = 0.1\sigma$) and using eq. (4). The agreement between the measured values and those predicted by the theoretical model is very good, confirming further that eq. (7) describes the creep behaviour of this alloy, at 673 K. In addition, preliminary observations of the microstructure by electron microscopy and studies of the evolution of the texture during creep confirm this conclusion [30].

Some comments should be made about the measured apparent activation energy, since this parameter has a physical significance only within a specific model. In fact, taking into account the definition of Q, on differentiating eq. (7) and rearranging terms, leads to

$$Q = U_d + U_j[4 - (6X + 3Y)/(1 + X)] + kT[2 - 3Y/(1 + X)], \quad (24)$$

where

$$X = \beta\left[1 + \beta^2(\dot{\epsilon}/\dot{\epsilon}^*)^{2/3}\right]^{-1/2},$$

$$Y = \alpha\sigma/(\dot{\epsilon}/\dot{\epsilon}^*)^{1/3}.$$

It was assumed in eqs. (8) to (12) that $l \sim \exp(U_j/kT)$, $c_j = \exp(-U_j/kT)$ and $D_v = D_0 \exp(-U_d/kT)$, where U_d is the energy (strictly the enthalpy) for self-diffusion and U_j is the energy to form a jog. Eq. (24) shows that $Q = U_d$ only if the last two terms are small. According to Gittus [15], however, Q lies between $U_d + U_j$ and $U_d - 2U_j$ and since U_j is much smaller than U_d, he concluded that the measured apparent activation energy for creep coincides with the energy for self-diffusion. On taking typical values for α, $\dot{\epsilon}^*$, β, σ and $\dot{\epsilon}$ (for example, the values given in table 3), however, it can be easily shown that eq. (24) reduces to

$$Q = U_d + U_j(-10 \text{ to } -20) + kT(-10). \quad (25)$$

Since $kT(673\ \text{K}) = 5.6$ kJ/mol and $U_j = Gb^3/8\pi = 21$ kJ/mol [see eq. (21)], it can be seen that the contribution due to the two last terms on the right hand side of eq. (25) cannot be ignored. This problem will be discussed in detail elsewhere [31], but it is clear that it cannot be simply stated, in this case, that $Q = U_d$ and, in fact, recent measurements of the self-diffusion coefficient by means of ion-beam-sputtering techniques, extrapolated to 673 K, give $U_d \approx 120$ kJ/mol [20]. This value differs substantially from the measured value for the apparent activation energy for creep (of the order of 300 kJ/mol).

Finally, it is clear that the meaning of the different parameters measured during creep experiments depends on the particular model considered. In fact, the steady-state regime, as defined in a strain versus time diagram, is mainly considered in the literature. When the data are viewed in a log σ–log $\dot{\epsilon}$ diagram, however, no separation is needed between the transient and steady-state regime. The steady-state regime can only be defined by a constancy of the parameters K and l and not by $\dot{\epsilon}$ = constant. Furthermore, as pointed out in the introduction, even in a log σ–log $\dot{\epsilon}$ diagram the data can be interpreted by using different models, as those expressed by eqs. (1) and (2). The model presented in this paper was preferred since a complete description of the creep and stress relaxation behaviour of Zircaloy-4, at 673 K, is possible and microstructural observations confirm the predictions of the model.

3. Conclusions

The creep characteristics of cold-worked and stress-relieved Zircaloy-4, at 673 K, are described by a model of diffusion controlled creep involving jog-drag and cell formation. The average distance between neighbouring jogs on dislocations and the ratio of cell diameter to dislocation spacing was obtained as a function of creep strain. The self-diffusion coefficient, calculated from the parameters obtained from the creep curves, was similar to the value measured by recent experiments utilizing

ion-beam-sputtering techniques. Finally, by a grain-counting technique, it was shown that grain boundary sliding gives only a small contribution to the creep strain, for the stresses and strain rate considered.

Acknowledgements

This work was performed within the Special Intergovernamental Agreement between Argentina and the Federal Republic of Germany and was supported in part by the "Proyecto Multinacional de Tecnología de Materiales" OAS-CNEA and the CIC.

Appendix

According to Gittus [15], during creep and at the equilibrium condition

$$\gamma = (K_1/r_b) - (r_b^2/2b)\dot{\epsilon}, \tag{A1}$$

where $\gamma = dr_b/dt$; r_b is the separation of dislocations in the cell wall and

$$K_1 = D_v G b^3 c_j / 2kT. \tag{A2}$$

Eq. (A1) can be rewritten as

$$r_b^3 + (\gamma/K_1) R_0^3 r_b - R_0^3 = 0, \tag{A3}$$

with

$$R_0^3 = 2bK_1/\dot{\epsilon}. \tag{A4}$$

The solution of the cubic eq. (A3) is

$$r_b = (bK_1/\dot{\epsilon})^{1/3}\left\{\left[1 + (1+x)^{1/2}\right]^{1/3} + \left[1 - (1+x)^{1/2}\right]^{1/3}\right\}, \tag{A5}$$

where

$$x = 8\gamma^3 b/27K_1^2\dot{\epsilon}. \tag{A6}$$

Furthermore, on taking into account that

$$(1+x)^{1/2} = 1 + \frac{x}{2} - \frac{x^2}{8} + \frac{x^3}{16} - \ldots \qquad -1 < x < 1,$$

and since $x \ll 1$ only the first term of the series expansion can be considered and eq. (A5) is reduced to

$$r_b = R_0\left[(1+y)^{1/3} - y^{1/3}\right], \tag{A7}$$

with

$$y = x/4. \tag{A8}$$

In addition, since

$$(1+y)^{1/3} = 1 + \frac{y}{3} - \frac{y^2}{9} + \ldots \qquad -1 < y < 1,$$

on taking only the first term of the series expansion eq. (A7) can be expressed as

$$r_b = R_0\left(1 + \frac{y}{3} - y^{1/3}\right), \tag{A9}$$

which, on considering eqs. (A6) and (A8) can be written as

$$r_b = R_0\left\{1 + R_0\frac{\gamma}{3K_1}\left[\tfrac{1}{3}(R_0/3K_1)^2 - 1\right]\right\}. \tag{A10}$$

Furthermore, if

$$\tfrac{1}{3}(R_0\gamma/3K_1)^2 \ll 1, \tag{A11}$$

eq. (A10) reduces to

$$r_b = R_0\left(1 - R_0\frac{\gamma}{3K_1}\right). \tag{A12}$$

On substituting eq. (A12) into eq. (A3) it is easy to show that the condition expressed by eq. (A11) leads to

$$R_0^6(\gamma/3K_1)^2 \approx 0. \tag{A13}$$

According to Gittus

$$F = \sigma - (Gb/K^2 r_b), \tag{A14}$$

$$\frac{\sigma - F}{G} = \left[\alpha A\dot{\epsilon}/\sinh(\alpha F)\right]^{1/2}, \tag{A15}$$

where F is the net stress causing the mobile dislocation to glide. On taking into account eq. (A12), eq. (A14) can be written as

$$\frac{\sigma - F}{G} = b/K^2 R_0(1 - \xi R_0), \tag{A16}$$

with

$$\xi = \gamma/3K_1. \tag{A17}$$

Equating eqs. (A15) and (A16), taking into account eq. (A4) and solving for F, lead to

$$F = \frac{1}{\alpha}\sinh^{-1}\left[AK^4G^2B\left(\frac{(\dot{\epsilon}/B)^{1/3} - \xi bG}{(\dot{\epsilon}/B)^{1/6}}\right)^2\right],$$

which, on making use of eq. (A15) gives

$$\sigma = \frac{1}{K^2}\left(\frac{(\dot{\epsilon}/B)^{2/3}}{(\dot{\epsilon}/B)^{1/3} - \Gamma}\right) + \frac{1}{\alpha}\sinh^{-1}\left[G^2K^4AB\alpha\left(\frac{(\dot{\epsilon}/B)^{1/3} - \Gamma}{(\dot{\epsilon}/B)^{1/6}}\right)^2\right], \tag{A18}$$

where

$$\Gamma = \frac{2}{3}\frac{\gamma b}{BG^2}.$$

At steady-state $\gamma = dr_b/dt = 0$, $\dot{\epsilon}$ = constant and $\Gamma = 0$

so that eq. (A18) reduces to eq. (7) of the text.

Finally, it is easy to show that for the range of stresses and strain rates shown in fig. 3. $\Gamma \ll (\dot{\epsilon}/B)^{1/3}$ and, consequently, eq. (7) also describes the transient regime in this case.

References

[1] G.E. Lucas, Thesis, MIT (1978).
[2] M. Novák and M. Hamerský, Czech. J. Phys. B 31 (1981) 338.
[3] S.R. MacEwen, R.G. Fleck, E.T.C. Ho and O.T. Woo, Metall. Trans. 12A (1981) 1751.
[4] R.L. Keusseyan, J. Wanagel, H. Ocken, J.T.A. Roberts and Che-Yu Li, J. Nucl. Mater. 98 (1981) 86.
[5] F. Povolo and A.J. Marzocca, J. Nucl. Mater. 97 (1981) 323.
[6] F. Povolo and A.J. Marzocca, J. Nucl. Mater. 98 (1981) 322.
[7] E.W. Hart, Che-Yu Li, H. Yamada and G.L. Wire, Constitutive Equations in Plasticity, ed., A.S. Argon (MIT Press, Cambridge, Ma, 1975) p. 149.
[8] E.W. Hart, J. Eng. Mater. Technol. 98 (1976) 193.
[9] C.R. Barrett and W.D. Nix, Acta Met. 13 (1965) 1247.
[10] F. Povolo and A.J. Marzocca, J. Nucl. Mater. 99 (1981) 317.
[11] F. Povolo and A.J. Marzocca, J. Mater. Sci. 18 (1983) 1426.
[12] F. Povolo and G.H. Rubiolo, J. Mater. Sci. 18 (1983) 821.
[13] F. Povolo and G.H. Rubiolo, Proc. 6th Int. Conf. on the Strength of Metals and Alloys, Melbourne, Australia (August 16-20, 1982), p. 589.
[14] W.A. Rachinger, J. Inst. Metals B1 (1952-53) 33.
[15] J.H. Gittus, Phil. Mag. 34 (1976) 401.
[16] F. Povolo, J. Nucl. Mater. 96 (1981) 178.
[17] F. Povolo, A.J. Marzocca and G.H. Rubiolo, Res Mech. (1983) in press.
[18] F. Povolo and P.N. Peszkin, Res Mech. 6 (1983) 233.
[19] F. Dyment and C. Libanati, J. Mater. Sci. 3 (1968) 349.
[20] F. Dyment, private communication.
[21] J. Friedel, Dislocations (Pergamon Press, London, 1964) p. 60.
[22] S. Takeuchi and A.S. Argon, J. Mater. Sci. 11 (1976) 1542.
[23] J.H. Gittus, Phil. Mag. 35 (1977) 293.
[24] D.L. Holt, J. Appl. Phys. 41 (1970) 3197.
[25] A. Orlova and J. Čádek, Phil. Mag. 28 (1973) 891.
[26] R. Horiuchi and M. Otsuka, Trans. Japan Inst. of Met. 13 (1972) 284.
[27] V.V. Levitin, V.I. Bobenko and A.L. Zletsin, Phys. Met. Metallogr. 35 (1973) 284.
[28] J.P. Poirier, Phil. Mag. 26 (1972) 713.
[29] M. Maeda, H. Oikawa and S. Kareskima, Scripta Met. 8 (1974) 183.
[30] F. Povolo, A.J. Marzocca and D. Hermida, to be published.
[31] F. Povolo and A.J. Marzocca, J. Nucl. Mater. (1983) in press.